

# The AGN and Gas Disk in the Low Surface Brightness Galaxy PGC 045080

M.Das<sup>1</sup>, N.Kantharia<sup>2</sup>, S.Ramya<sup>3</sup>, T.P.Prabhu<sup>3</sup>, S.S.McGaugh<sup>4</sup>, S.N.Vogel<sup>4</sup>

*1.Raman Research Institute, Bangalore, 560080, India*

*2.National Centre for Radio Astrophysics, Tata Institute of Fundamental Research, Post Bag 3, Ganeshkhind, Post Bag 3, Ganeshkhind, Pune - 41100*

*3.Indian Institute of Astrophysics, Koramangala, Bangalore, India*

*4.Department of Astronomy, University of Maryland, College Park, MD 20742, USA*

*(E-mails:mousumi@rri.res.in)*

Accepted.....; Received .....

## ABSTRACT

We present radio observations and optical spectroscopy of the giant low surface brightness (LSB) galaxy PGC 045080 (or 1300+0144). PGC 045080 is a moderately distant galaxy having a highly inclined optical disk and massive HI gas content. Radio continuum observations of the galaxy were carried out at 320 MHz, 610 MHz and 1.4 GHz. Continuum emission was detected and mapped in the galaxy. The emission appears extended over the inner disk at all three frequencies. At 1.4 GHz and 610 MHz it appears to have two distinct lobes. We also did optical spectroscopy of the galaxy nucleus; the spectrum did not show any strong emission lines associated with AGN activity but the presence of a weak AGN cannot be ruled out. Furthermore, comparison of the H $\alpha$  flux and radio continuum at 1.4 GHz suggests that a significant fraction of the emission is non-thermal in nature. Hence we conclude that a weak or hidden AGN may be present in PGC 045080. The extended radio emission represents lobes/jets from the AGN. These observations show that although LSB galaxies are metal poor and have very little star formation, their centers can host significant AGN activity. We also mapped the HI gas disk and velocity field in PGC 045080. The HI disk extends well beyond the optical disk and appears warped. In the HI intensity maps, the disk appears distinctly lopsided. The velocity field is disturbed on the lopsided side of the disk but is fairly uniform in the other half. We derived the HI rotation curve for the galaxy from the velocity field. The rotation curve has a flat rotation speed of  $\sim 190\text{km s}^{-1}$ .

**Key words:** Galaxies:spiral - Galaxies:individual - Galaxies:nuclei - Galaxies:active - Galaxies:jets Galaxies: ISM - Galaxies:kinematics and dynamics

## 1 INTRODUCTION

Low surface brightness (LSB) galaxies have diffuse stellar disks, large HI disks and low metallicities (Impey & Bothun 1997; Bothun et al. 1997). They are poor in star formation which is usually localized to relatively small patches over their disks (McGaugh 1994; de Blok & van der Hulst 1998; Kuzio de Naray et al. 2004). Very few LSB galaxies have been detected in molecular gas, which is a fairly reliable indicator of the star forming potential in a galaxy ((O’Neil, Hofner & Schinnerer 2000; Matthews & Gao 2001; O’Neil, Schinnerer & Hofner 2003; Matthews et al. 2005; Das et al. 2006). The combined low star formation rates and metallicities of these galaxies suggest that they are less evolved compared to high surface brightness (HSB) galaxies (McGaugh & Bothun 1994; de Blok et al. 1995). They are in some sense more "primordial" than their HSB counterparts.

One of the reasons for the lack of evolution could be the massive dark halos that dominate the disks of these galaxies (e.g. de Blok & McGaugh 1997). Dark matter halos inhibit the growth of disk instabilities such as bars and spiral arms which can act as triggers of large scale star formation in galaxies and help propel their evolution (Mihos, McGaugh & de Blok 1997).

Recent studies indicate that LSB galaxies span a wide range of morphologies from the more populous dwarf spiral/irregular galaxies to the large spirals like Malin 1 (McGaugh, Schombert & Bothun 1995; Galaz et al. 2002). The large LSB galaxies or the so called giants are relatively rarer than the smaller LSB galaxies (Bothun et al. 1990; Sprayberry et al. 1995). Many giant LSB galaxies have large bulges associated with extended diffuse stellar disks (Beijersbergen et al. 1999). Although their disks are faint, they often show

a distinct spiral structure (e.g. UGC 6614; Pickering et al. 1997) and in some rare cases are even barred (e.g. UGC 7321; Pohlen et al. 2003).

The optical spectrum of many LSB giants show emission lines characteristic of an active galactic nucleus (Sprayberry et al. 1993; Schombert 1998). This is surprising as AGNs are usually associated with optically bright galaxies that are undergoing significant star formation (Ho, Philippenko & Sargent 1997). At least 20% of LSB galaxies show spectroscopic signs of AGN activity (Impey, Burkholder & Sprayberry 2001). However, detailed investigations of the AGN activity at wavelengths other than optical have not been done. A handful of giant LSB galaxies are bright at radio frequencies in the NVSS and FIRST VLA surveys (e.g. UGC 1922 in O’Neil & Schinnerer 2004) but deeper observations are lacking. Das et al. (2006) detected a millimeter continuum source in UGC 6614; the emission is flat spectrum between 1.4 to 110 GHz and is due to the AGN in the galaxy. These results suggest that the AGN in LSB galaxies may have similar properties compared to HSB galaxies even though their evolutionary histories are very different.

We have undertaken a radio study of several giant LSB galaxies with the Giant Meterwave Radio Telescope (GMRT) at metre wavelengths. This paper on PGC 045080 is the first in this study. We have also done optical spectroscopy of the nucleus using the Himalayan Chandra Telescope (HCT). In the following sections we present an overview of the galaxy, the HCT observations, the GMRT radio observations and our results. Finally we discuss the implications of our observations. As PGC 045080 has a moderately high redshift ( $z=0.0409$ ) we will adopt a luminosity distance of  $D_L = 176.4 \text{ Mpc}$  ( $H_0 = 71 \text{ km s}^{-1} \text{ Mpc}^{-1}$ ) which leads to a distance scale of  $0.86 \text{ kpc arcsec}^{-1}$ .

## 2 THE LSB GALAXY PGC 045080

PGC 045080 is a fairly isolated giant LSB galaxy. The main properties of the galaxy are listed in Table 1. The galaxy is close to edge on, has a faint nucleus and very low surface brightness disk. An oval structure is visible in the galaxy center and may represent a weak bar or a bulge. Although highly inclined, spiral arms are clearly visible in the galaxy disk. The optical spectrum of PGC 045080 was observed by Sprayberry et al. (1995) as part of a larger study of the nuclei of giant LSB galaxies. Although they found signatures of AGN activity in several other LSB galaxies, they did not find AGN activity in PGC 045080. However, their spectral resolution was rather poor and weak AGN activity may have been missed.

As in most LSB galaxies the neutral hydrogen (HI) content of the galaxy is high compared to its stellar mass. Single dish observations indicate that the HI gas disk has a double horned profile typical of a rotating gas disk (Sprayberry et al. 1995; Matthews et al. 2001). The HI mass is  $\sim 10^{10} M_\odot$  for this galaxy (Impey, Burkholder & Sprayberry 2001). However, neither the HI gas distribution nor disk kinematics in 4 have been mapped before.

## 3 GMRT RADIO OBSERVATIONS

We observed 4 with the GMRT on four days from August 2005 to March 2006. The details of the observations are listed in Table 2. The GMRT is an array of thirty antennas of 45m diameter each; 14 antennas are arranged in a central compact array and the remaining are distributed over a Y shaped configuration (Swarup et al. 1999; Ananthakrishnan & Rao 2002). Nearby radio source were used for phase calibration. The data was obtained in the native “lta” format, converted to FITS format and then analysed using AIPS<sup>1</sup>.

Continuum observations were done at frequencies 1.4 GHz, 610 MHz and 325 MHz. Bad data on a single channel on the amplitude and bandpass calibrator were iteratively edited and calibrated until satisfactory gain solutions were obtained using standard tasks in AIPS. This was used to generate bandpass solutions. The central 85 channels were bandpass calibrated and averaged to obtain the continuum database. This was then imaged using IMAGR. Several nearby bright sources were used to self calibrate the continuum images. A relatively bright point source lies approximately  $2'$  to the north west of PGC 045080; the source is seen in the FIRST and NVSS VLA maps and has a peak flux of  $\sim 80 \text{ mJy}$ . The presence of this bright source limited the sensitivity of the map close to the galaxy. Wide field imaging was used at 610 MHz and 325 MHz; at 610 MHz the primary beam was divided into 9 facets and at 325 MHz it was divided into 25 facets. At all frequencies both natural and uniform weighted maps of PGC 045080 were made.

For the HI line observations, the data were also gain and bandpass calibrated. The HI data cube was generated from the UV line data using a maximum UV distance of 40 Klambda. Since a bandwidth of 8 MHz was used for the observations, the resulting resolution was 62.5 KHz or  $14.3 \text{ km s}^{-1}$ . The task MOMNT in AIPS was then used to generate moment maps from the data cube using a cutoff of  $1.2 \text{ mJy/beam}$  (i.e.  $2\sigma$ ). These maps reveal the HI intensity distribution and the gas kinematics in the galaxy disk. The velocity field was also used to derive the HI rotation curve; this was done using the program rotcur which is part of the software toolbox NEMO (Teuben 2001). Rotcur uses the tilted ring analysis of Begeman (1989). The HI disk was divided into annuli and the velocity averaged for each ring. Nyquist sampling was used to maximize the number of annuli sampled. We used rotcur to find a dynamical center for the galaxy; it is offset by approximately  $1''$  from the SDSS optical center of the galaxy.

## 4 RESULTS OF RADIO OBSERVATIONS

Radio continuum emission from this galaxy was detected for the first time. In previous VLA observations at 1.4 GHz (NVSS maps; Condon et al. 1998), the galaxy falls below NVSS detection limits, although there is a peak in the NVSS map at the  $2\sigma$  level. The galaxy is not detected in the higher resolution FIRST survey (Becker, White & Helfand 1995). However both surveys did not go very deep. Using the

<sup>1</sup> AIPS is distributed by NRAO which is a facility of NSF and operated under cooperative agreement by Associated Universities, Inc.

GMRT we have detected radio continuum emission from the center of PGC 045080 at all three frequencies i.e. 1.4 GHz, 610 MHz and 325 MHz. Apart from radio continuum observations, we have also mapped the HI gas distribution in the galaxy. Previous HI observations were all single dish and did not give any informations about the gas morphology or kinematics. In the following paragraphs we discuss our results in more detail; the flux estimates and beams have been summarised in Table 3.

#### 4.1 RADIO CONTINUUM OBSERVATIONS

(i) **1.4 GHz** The distribution of the 1.4 GHz radio continuum emission is shown in Figures 1 to 4. Figure 1 shows the high sensitivity map made with natural weighting. The resolution is rather poor (beam  $\sim 8''$ ) but the extended flux distribution is clearly seen. There is a peak in the flux distribution that has a S/N ratio of 8 and is offset from the nucleus of the galaxy by  $1 - 2''$ . The peak flux of the emission is  $\sim 0.71 \text{ mJy beam}^{-1}$  and it extends over a region  $\sim 10'' - 15''$  in size. The emission also has a southern spur like feature (Figure 2). This is clearer in the higher resolution map made with uniform weighting (Figure 3 and 4), where the southern extension has a S/N 4 but does not appear to be associated with the galaxy. At 610 MHz this low level emission extending south of the galaxy falls below the  $2\sigma$  level. Hence it is unlikely to be nonthermal in nature and associated with a background galaxy. It is also unlikely to be due to star formation as there is no emission associated with it in the optical images (Sprayberry et al. 1995); thus the emission extending to the south may not be real.

At high resolution (beam  $\sim 4.3''$ ) in Figure 3 the 1.4 GHz emission breaks up into two main cores. The galaxy center lies closer to the brighter peak but does not lie exactly between the two peaks (Figure 4). Hence from this map it is not clear whether the emission has a double lobe structure about the nucleus or not. However, at both resolutions the emission lies along an axis which is slightly offset from the optical axis of the galaxy. This suggests that the continuum emission may not be due to star formation in the galaxy disk but instead may be associated with an AGN in the galaxy. If so, then the extended emission may be jets or lobes originating from the active nucleus. This is discussed in more detail in Section 7.

(ii) **610 MHz** Figure 5 shows the radio continuum emission from PGC 045080 at 610 MHz. This is the low resolution but high sensitivity map made with natural weighting. The emission has an extended structure as in the 1.4 GHz emission map (Figures 1 to 4). The emission peaks on one side of the galaxy and the peak has a S/N ratio of 6. The emission extends over  $\sim 15''$  and the peak flux is  $\sim 0.88 \text{ mJy beam}^{-1}$  where the beam is  $\sim 10''$ . In the higher resolution map made with uniform weighting, the extended emission breaks up into two lobes about the center of the galaxy (Figure 6). Both high and low resolution maps suggest a double lobed morphology for the emission and the lobe east of the galaxy center is possibly the closer lobe as it appears brighter in both the high and low resolution maps.

(iii) **325 MHz** At 325 MHz the galaxy is detected in the radio continuum with a S/N of 4 but the map is noisy and the resolution is poor. Hence not much can be said about

the structure except that it is extended. The peak flux in the map is  $\sim 3.56 \text{ mJy beam}^{-1}$  where the beam  $\sim 13''$ .

(iv) **Spectral Index** The radio maps of PGC 045080 are too noisy to derive meaningful spectral index maps. So instead we used the peak flux in the 1.4 GHz and 325 MHz maps to calculate the spectral index. We obtained a value of  $\alpha = -0.63 \pm 0.2$  where  $\alpha$  is defined as  $S_\nu \propto \nu^\alpha$ . Within error limits the spectral index is what is expected from either star forming regions or jets associated with an active nucleus.

#### 4.2 HI GAS DISK

Although the HI content of PGC 045080 had been studied earlier in single dish observations, the gas distribution had not been studied. Hence this is the first HI map of this galaxy. The results of our GMRT HI line observations of PGC 045080 are discussed below.

(i) **HI disk size and mass:** The most striking feature of the HI distribution in PGC 045080 is its extent compared to its stellar disk. Figure 7 shows the HI intensity map of PGC 045080 and Figure 8 shows the intensity contours overlaid on the SDSS R band optical image of the galaxy. The gas disk is about twice the size of the optical disk and possibly much thicker as well. The optical disk has a diameter of approximately  $40''$  whereas the gas disk has a diameter of  $80''$ . A larger HI disk relative to the optical disk is typical in LSB galaxies (Pickering et al. 1997). But it is more clearly seen in this galaxy as it is nearly edge on. The total HI flux is  $\sim 0.86 \text{ Jy kms}^{-1}$  which leads to a HI gas mass of  $6.3 \times 10^9 M_\odot$ . This is approximately two thirds of the single dish HI flux observed with the Arecibo telescope by Sprayberry et al. (1995) which is  $9.6 \times 10^9$ . The difference is probably because of the limitation in uv space coverage in our GMRT observations (although we had 2 tracks of data on this galaxy, only one data set was included in the channel map because data quality of the second days observation was poor). Assuming that the HI gas disk has a radius  $\sim 40''$ , the mean surface density of HI is  $\Sigma \sim 1.7 M_\odot pc^{-2}$ . This is lower than that observed in other giant LSB galaxies; for example UGC 6614 has a corresponding value of  $\Sigma \sim 3.2 M_\odot pc^{-2}$  (Pickering et al. 1997).

(ii) **Lopsided HI distribution:** The HI intensity distribution on either side of the galaxy nucleus is different and gives the galaxy a "lopsided" appearance. The peak HI intensity east of the nucleus in the disk is about 1.4 times the peak on the west. The lopsided nature of the HI disk peaks just at the edge of the optical disk ( $\sim 17''$ ). One side of the disk is also more flared indicating that the HI disk is perhaps warped. A warped disk has also been seen in a more prominent LSB galaxy, Malin 1 (Pickering et al. 1997).

(iii) **Minimum in HI distribution:** There is a dip in the HI intensity on brighter side of PGC 045080 near the galaxy center; the origin of the HI dip is not clear as there is no bright star formation in this region. However, it may however be related to the extended radio continuum emission observed in the galaxy because the peak emission of the lobe east of galaxy center is close to the dip in HI intensity. Figure 9 shows the 610 MHz map contours overlaid on the HI map. Note that the brighter lobe that lies east of the galactic center coincides with the dip in the HI intensity. This indicates that there may have been some disk-jet in-

teraction that resulted in some of the HI being evaporated away leaving behind a dip in the gas distribution.

**(iv) HI velocity field:** The intensity weighted velocity field or moment 1 map of HI disk is shown in Figure 10. The velocity contours on one side of the disk (west of nucleus) look fairly typical of a rotating disk. But the velocity field on the other side (i.e. the flared half of the disk) is not uniform. This again suggests that the HI disk is warped or lopsided and hence the velocity field is non-symmetric about the galaxy center.

**(v) HI Rotation Curve:** The intensity weighted velocity field was used to derive the HI rotation curve for the galaxy. As discussed earlier in Section 5 we used rotur to determine a dynamical center for the galaxy and it is offset by approximately  $1''$  from the SDSS center of the galaxy. We plotted the rotation curves for the approaching and receding sides separately (Figure 11). The two curves are significantly different in the inner  $15''$  radius of the disk, but have similar speeds in the outer region. The two curves were averaged to obtain the mean rotation curve for the galaxy (Figure 12). The curve is relatively flat until a radius of approximately  $35''$ ; beyond that it starts rising. At radii larger than  $\sim 45''$  there is not much gas and hence not enough points to fit a reliable rotation curve. The flat rotation speed for 4 is  $\sim 190 \text{ km s}^{-1}$ .

## 5 HCT OPTICAL OBSERVATIONS

The radio continuum observations discussed in Section 4.1 suggest the presence of an AGN in PGC 045080. In particular the double lobed structure seen in the 610 MHz map (Figure 6) is often observed in galaxies harboring radio loud AGNs. To get a better understanding of the nuclear activity in PGC 045080 we did optical spectroscopy of the galaxy nucleus with the HCT, which is a 2m optical telescope located in the Hanle valley in Ladakh. Long slit spectroscopic observations of the central bright nucleus were obtained on 29th and 30th April, 2006. We used a 1671 slit (dimensions  $1.92'' \times 11'$ ) and a combinations of two grisms, Grism 7 (3800 to 6840 Å) which has a resolution of  $1.45 \text{ Å pixel}^{-1}$  and Grism 8 (5800 to 8350 Å) which has a resolution of  $1.25 \text{ Å pixel}^{-1}$ . The exposures in both the grisms was one hour each on both nights. For wavelength calibration we observed Fe-Ar and Fe-Ne calibration lamps for a few seconds each. Flux calibration was done by observing the standard star Feige 34.

The nuclear spectrum was extracted over  $8.88''$  length along the slit. Since the nights were not photometric, the continuum fluxes obtained for the two nights differed. So we used the SDSS spectrum of this galaxy as a secondary calibrator to scale the flux levels and fit the continuum shape. Data reduction was done using IRAF<sup>2</sup> with the task APALL in the SPECRED package. The task FITPROFS was used to deblend the spectral lines and derive the total flux, equivalent widths and FWHM of the lines.

<sup>2</sup> IRAF is distributed by the NOAO which is operated by AURA under cooperative agreement with NSF.

## 6 RESULTS OF OPTICAL SPECTROSCOPY

The final spectrum is shown in Figure 13 and the details of the emission lines are listed in Table 4. The spectrum has a narrow but prominent  $H\alpha$  line and strong [SII] and [NII] lines in emission. The emission lines are superimposed on a stellar continuum and absorption line spectrum. The  $H\beta$  and  $H\gamma$  lines are seen in absorption suggesting significant star formation has taken place in recent past. The signatures of older population are also evident making it difficult to model the star-formation history. We could not identify any strong emission lines indicative of AGN, such as broad  $H\alpha$  and high excitation lines such as [OIII], HeII and lines of Ne. The intermediate excitation lines of [FeVI] 5158Å and [FeVII] 6058Å are detectable. However, they can arise due to AGN as well as SN II in the post-starburst phase. Thus the optical spectrum of the galaxy nucleus does not provide an unambiguous signature of AGN in PGC 045080.

We also used the flux values of the emission lines to determine the position of PGC 045080 on the AGN diagnostic diagrams (Baldwin et al. 1981). The diagnostic diagrams provide a very good tool to distinguish between AGN and starburst emission in galaxies (Groves, Heckman, Kauffman 2006; Kewley et al. 2006). Figure 14 shows the plot of  $\log(\text{O[III]}/H\beta)$  against  $\log(\text{[NII]}/H\alpha)$ . The solid line is the limit for extreme starburst regions from Kewley et al. (2001) and the dashed line is the lower limit between AGN and starburst nuclei from Kauffman et al. (2003). The region between these two lines forms the composite region where the spectra may contain contributions from both AGN and starburst emission. PGC 045080 lies on the dashed line and is hence on the boundary between HII regions and AGN/starburst nuclei. The low value of  $\text{O[III]}/H\beta$  excludes a Seyfert type nucleus, and at most a weak LINER may contribute to the optical spectrum. To summarise, the emission line spectrum of the nucleus does not show any clear signatures of AGN activity. At most the AGN may be a weak LINER that is visible at radio frequencies but not in the optical.

## 7 IS THERE AN AGN IN PGC 045080?

We have done radio observations and optical spectroscopy of the nucleus of PGC 045080. Extended radio continuum emission was detected from the galaxy at 1.4 GHz, 610 MHz and 325 MHz. The emission morphology suggests that it is not associated with star formation in the disk but may instead be due to AGN activity. Optical spectroscopy of the nucleus was done to see if the spectrum had emission lines characteristic of an AGN. However as discussed in Section 6 we did not see any outstanding emission lines in the optical spectrum that confirms the presence of an AGN in PGC 045080. The  $H\alpha$  line is prominent but narrow and the O[III] line is relatively weak. Considering its position on the diagnostic diagram we conclude that at most there may be a weak AGN in the galaxy and it may host LINER type activity. However another approach is to compare the expected radio continuum from  $H\alpha$  flux with that actually observed at 1.4 GHz. We used only the  $H\alpha$  flux from the nuclear region over a slit dimension of  $1.92'' \times 8.88''$ . Assuming that the strong  $H\alpha$  line arises from star formation, we corrected the spectrum

for reddening using the standard balmer decrement method used by Kong et al. (2002), wherein the intrinsic theoretical  $H\alpha/H\beta$  is assumed to be 2.87 for starburst galaxies. The  $E(B-V)$  for this galaxy is then 0.153 magnitude. After correcting for reddening, the nuclear  $H\alpha$  luminosity amounts to  $2.09 \times 10^{40}$  erg s<sup>-1</sup>. This is an upper limit for the expected  $H\alpha$  flux from star formation. The resulting infrared flux is  $\sim 1.18$  erg s<sup>-1</sup>cm<sup>-2</sup> (Kennicutt 1998) and the expected radio continuum emission at 1.4 GHz from nuclear star formation is 0.23 mJy (Condon et al. 2002). We then used the GMRT radio continuum map (Figure 1) to determine the 1.4 GHz flux from PGC 045080 over a region similar to that of the optical slit used in the HCT observations. This was done to compare as precisely as possible the expected radio flux from star formation with that actually observed in the GMRT maps. The integrated flux over the nuclear region is 0.54 mJy which is more than two times that expected from star formation. Hence a significant fraction of the radio continuum emission from PGC 045080 is non-thermal in nature and is most likely due to an AGN in the galaxy. Also, there is no significant  $H\alpha$  flux detected from the disk in the spectrum; the  $H\alpha$  emission arises mainly from the nucleus. (This is clear when we compared the  $H\alpha$  emission from the slit integrated over the disk with that over the nucleus). This further supports the idea that the extended radio continuum is non-thermal in nature and is associated with an AGN in the galaxy.

## 8 DISCUSSION

We have done radio observations and optical spectroscopy of the nucleus of PGC 045080. Extended radio continuum emission was detected from the galaxy at 1.4 GHz, 610 MHz and 325 MHz. We also mapped the extended HI gas distribution and velocity field in the galaxy. In the following section we discuss the implications of our observations.

**(i) Radio Jets in PGC 045080:** If the radio continuum is from an AGN in the galaxy, the morphology suggests that we are detecting only the radio jets or lobes and not the core. This is not unusual and is seen in more powerful radio galaxies as well (e.g. NGC 3801, Das et al. 2005). The core emission is self absorbed and becomes visible only at higher frequencies. From the higher resolution maps at 1.4 GHz and 610 MHz it is clear that the radio lobe lying east of the nucleus is brighter than that on the west. The galaxy center is also marginally closer to the brighter lobe. This may indicate that the lobe to the east is closer to us than that on the western side. However since the resolution is poor, details of the galaxy and radio lobe morphology are difficult to understand. Higher resolution observations are required to fully understand the radio jet/lobe morphology.

**(ii) Radio Power in Jets :** Assuming that the extended emission is mainly non-thermal in nature, we can calculate the radio power in the lobes and compare it with other radio sources. Using the formula for equipartition of energy between magnetic fields and particle energies (Longair 1983) the total energy in synchrotron emission in the lobes (assuming a frequency of 325 MHz) is  $\sim 1.5 \times 10^{55}$  erg. This is similar to the energy stored in compact cores or jets in Seyfert galaxies and also in FR I type radio sources. Hence these observations indicate that though LSB galaxies have a low

star formation rate, they can host AGN activity comparable to bright spirals and even radio galaxies. How AGN activity developed in these poorly evolved, low surface brightness galaxies is something we need to understand.

**(iii) Lopsided HI gas disk :** PGC 045080 is clearly asymmetric in the HI maps and to some degree in the optical image as well. Spiral galaxies have been found to be lopsided both in HI (Baldwin et al. 1980; Richter & Sancisi 1994) and in the near-infrared (Rix & Zaritsky 1995; Zaritsky & Rix 1997). The origin for the asymmetry can be due to ram pressure in a cluster environment or due to interactions with nearby galaxies (e.g. Angiras et al. 2006). It can also be due to an off center galaxy potential (Jog 1997; Levine & Sparke 1998) or slow gas accretion (Bournaud et al. 2005). Lopsidedness is also more commonly seen in late type galaxies, which are generally more halo dominated in their inner disks than early type galaxies (Matthews et al. 1998). Although PGC 045080 is a relatively isolated galaxy, it appears distinctly lopsided in the HI moment maps (Figures 7, 8 and 10). It also appears slightly asymmetric in the R band SDSS optical image, although it is difficult to tell as the galaxy is nearly edge on. Considering that PGC 045080 is a LSB galaxy and possibly has a massive dark halo, the most probable explanation for its lopsidedness is that its disk and halo potentials are off center with respect to each other (Noordermeer et al. 2001). Its also likely that a significant fraction of LSB galaxies are lopsided in their HI distribution as seen in the LSB dwarf galaxy DD0 9 (Swaters et al. 1999).

## 9 CONCLUSIONS

We have done an optical and radio study of the relatively distant LSB galaxy PGC 045080. The main results of our work are listed below.

**(i) Optical Spectrum :** The emission lines in the optical spectrum do not indicate the presence of strong AGN activity (i.e. a Seyfert type nucleus). At most a LINER type nucleus may be present.

**(ii) Extended Radio Continuum Emission :** We detected extended radio continuum emission from the galaxy at 1.4 GHz, 610 MHz and 320 MHz. The spectral index is  $\alpha = -0.63 \pm 0.2$ . The radio morphology suggests that the emission is not due to star formation but instead represents lobes or jets associated with an AGN in the galaxy.

**(iii) AGN and radio jets in the galaxy :** We compared the radio flux expected from the  $H\alpha$  emission to that actually observed at 1.4 GHz. We found that a significant fraction of the emission is non-thermal in nature and probably due to AGN activity in the galaxy. If so, then the extended radio continuum observed at 1.4 GHz and 610 MHz are radio lobes associated with the AGN. Such structures have not been seen before in LSB galaxies. It suggests that these galaxies may harbour AGN that have radio properties similar to Seyfert galaxies.

**(iv) HI morphology and kinematics :** The HI disk extends out to approximately twice the optical size of the galaxy. The HI morphology is asymmetric w.r.t the galaxy center and appears thicker on the eastern side compared to the other half. The disk kinematics are also less regular in the flared or warped side compared to the more regularly ro-

tating western half. The rotation curve yields a flat rotation velocity of  $\sim 190\text{km s}^{-1}$ .

**(v) Lopsided HI disk :** The HI gas disk appears to be lopsided in the moment maps. As PGC 045080 is a fairly isolated galaxy, we think that the asymmetry may be due to an offset between the center of the disk and dark matter halo in the galaxy.

## 10 ACKNOWLEDGMENTS

We are grateful to the members of the GMRT staff for their help in the radio observations. The GMRT is operated by the National Centre for Radio Astrophysics of the Tata Institute of Fundamental Research. We thank the staff of IAO, Hanle and CREST, Hosakote, that made these observations possible. The facilities at IAO and CREST are operated by the Indian Institute of Astrophysics, Bangalore. This paper has used an SDSS image; funding for the SDSS and SDSS-II has been provided by the Alfred P. Sloan Foundation, the Participating Institutions, NSF, the U.S. Department of Energy, NASA, the Japanese Monbukagakusho, the Max Planck Society, and the Higher Education Funding Council for England. This research has made use of the NASA/IPAC Infrared Science Archive, which is operated by the JPL, California Institute of Technology, under contract with NASA.

## REFERENCES

- Ananthakrishnan, S., Rao, P., Multicolor Universe, eds. Manchanda & Paul
- Angiras, R. A., Jog, C. J., Omar, A., Dwarakanath, K. S. 2006, MNRAS, 369, 1849
- Baldwin, J. E., Lynden-Bell, D., Sancisi, R. 1980, MNRAS, 193, 313
- Becker, R.H., White, R.L., Helfand, D.J. 1995, ApJ, 450, 559
- Begeman, K. G., 1989, A&A, 223, 47
- Beijersbergen, M., de Blok, W. J. G., van der Hulst, J. M., 1999, A&A, 351, 903
- Bournaud, F., Combes, F., Jog, C. J., Puerari, I. 2005, A&A, 438, 507
- Bothun, G.D., Schombert, J.M., Impey, C.D., Schneider, S.E., 1990, ApJ, 360, 427
- Bothun, G., Impey, C., McGaugh, S.S. 1997, PASP, 109, 745
- Condon, J.J., Cotton, W.D., Broderick, J.J., 2002, AJ, 124, 675
- Condon, J.J., Cotton, W.D., Greisen, E.W., Yin, Q.F., Perley, R.A., Taylor, G.B., Broderick, J. 1998, AJ, 115, 1693
- Das, M., Vogel, S.N., Verdoes Kleijn, G.A., O’Dea, C.P., Baum, S.A., ApJ, 2005, 629, 757
- Das, M., O’Neil, K., Vogel, S.N., McGaugh, S.S., 2006, ApJ, 651, 853
- de Blok, W. J. G., van der Hulst, J. M., Bothun, G., 1995, MNRAS, 274, 235
- de Blok, W. J. G. & McGaugh, S.S., 1997, MNRAS, 290, 533
- de Blok, W. J. G. & van der Hulst, J. M. 1998, A&A, 336, 49
- de Naray, R.K., McGaugh, S.S., de Blok, W. J. G., 2004, MNRAS, 355, 887
- Galaz, G., Dalcanton, J.J., Infante, L., Treister, E., 2002, AJ, 124, 1360
- Groves, B.A., Heckman, T.M., Kauffmann, G., 2006, MNRAS, 371, 1559
- Ho, L.C., Filippenko, A.V., & Sargent, W.L.W., 1997, ApJ, 487, 568
- Impey, C. & Bothun, G. 1997, ARA&A, 35, 267
- Impey, C., Burkholder, V., Sprayberry, D., 2001, AJ, 122, 2341
- Jog, C.J. 1997, ApJ, 488, 642
- Kauffmann, G. et al., 2003, 2003, MNRAS, 346, 1055
- Kennicutt, R.C., 1998, ARA&A, 36, 189
- Kewley, L.J., Groves, B., Kauffmann, G., Heckman, T., 2006, MNRAS, 372, 961
- Kong, X., Cheng, F. Z., Weiss, A., Charlot, S., 2002, A&A, 396
- Levine, S.E., Sparke, L.S. 1998, 1998, ApJ, 496, L13
- Matthews, L. D., van Driel, W., Gallagher, J.S. III 1998, AJ, 116, 1169
- Matthews, L.D. & Gao, Y. 2001, ApJ 549, L191
- Matthews, L.D.; Gao, Y.; Uson, J.M.; Combes, F. 2005, AJ, 129, 1849
- McGaugh, S.S. 1994, ApJ, 426, 135
- McGaugh, S.S. & Bothun, G.D. 1994, AJ, 107, 530
- McGaugh, S.S., Schombert, J.M. & Bothun, G.D. 1995, AJ, 109, 2019
- Mihos, J. C., McGaugh, S.S., de Blok, W. J. G., 1997, ApJ, 477, L79
- Noordermeer, E., Sparke, L.S., Levine, S.E. 2001, MNRAS, 328, 1064
- O’Neil, K., Hofner, P., & Schinnerer, E. 2000, ApJ, 545, L102
- O’Neil, K., Schinnerer, E., & Hofner, P. 2003, ApJ, 588, 230
- O’Neil, K. & Schinnerer, E., 2004, ApJL 615, 109
- Pickering, T. E., Impey, C. D., van Gorkom, J. H., Bothun, G. D., 1997, AJ, 114, 1858
- Pohlen, M., Balcells, M., Ltticke, R., Dettmar, R.-J., 2003, A&A, 409, 485
- Richter, O.-G., Sancisi, R. 1994, A&A, 290, L9
- Rix, H., Zaritsky, D. 1995, ApJ, 447, 82
- Schombert, J.M., 1998, AJ, 116, 1650
- Sprayberry, D., Impey, C. D., Irwin, M. J., McMahon, R. G., Bothun, G. D., 1993, ApJ, 417, 114
- Sprayberry, D., Impey, C. D., Bothun, G. D., Irwin, M. J., 1995, AJ, 109, 558
- Swarup, G., Ananthakrishnan, S., kapahi, V., et al. 1991, current Science, 60, 95
- Swaters, R.A., Schoenmakers, R.H.M., Sancisi, R., van Albada, T.S. 1999, MNRAS, 304, 330
- Teuben, P., 1995, ASP Conf. Ser., 77, 398
- Zaritsky, D., Rix, H. 1997, ApJ, 477, 118

**Table 1.** Parameters of PGC 045080

Parameter	Value	Comment
Galaxy Type	Sc(f)	NED
Galaxy Position (RA, DEC)	13:03:16.0 +01:28:07	2MASS
Other Names	1300+0144, CGCG 015-059	
Velocity & Redshift	12,264 km s <sup>-1</sup> , 0.040908	NED
Luminosity Distance	176.4 Mpc	
Linear Distance Scale	0.86 kpc/arcsec	
Disk Inclination	71°	Sprayberry et al. 1995
Disk Optical Size ( $D_{25}$ )	0.55'	Sprayberry et al. 1995
Galaxy Position Angle (P.A.)	85°	2MASS

**Table 2.** Details of GMRT Observations

Name of Record	HI line	1.4 GHz	610 MHz	325 MHz
Date of Observation	19, 20 August 2005	19 August 2005	17 March 2006	12 December 2005
Central Frequency	1364.4 MHz	1364.4 MHz	604.5 MHz	317.6 MHz
Bandwidth	5.4 MHz	5.4 MHz	8.7 MHz	12.5 MHz
Phase Calibrator	1347+122	1347+122	1419+064	1419+064
Amplitude Calibrator	3C147, 3C286	3C147, 3C286	3C147	3C147, 3C286
Bandpass Calibrator	3C147, 3C286	3C147, 3C286	3C147	1419+064
Onsource Time	10 hours	6.5 hours	5.5 hours	3 hours
Band Center (HI Line)	12,264 km s <sup>-1</sup>	.....	.....	.....
Spectral Resolution	14.3 km s <sup>-1</sup> (62.5 kHz)	.....	.....	.....
Beam Size (Natural Weight)	14.7'' × 12.0''	8.4'' × 7.6''	11.7'' × 9.0''	14.5'' × 11.6''

**Table 3.** Results of Radio Continuum Observations of PGC 045080

Name of Record	1.4 GHz	610 MHz	325 MHz
Peak Flux ( $mJy beam^{-1}$ )	0.71	0.88	3.6
Noise	0.08	0.15	0.9
Beam Size (Natural Weight)	8.4'' × 7.6''	11.7'' × 9.0''	14.5'' × 11.6''

**Table 4.** Results of Optical Observations

Emission Line	Central Wavelength (Å°)	Flux (erg cm <sup>2</sup> s <sup>-1</sup> )	Equivalent Width (Å°)	FWHM (Å°)
H <sub>β</sub> (emission)	4862.178	1.707E-15	3.818	11.23
H <sub>β</sub> (absorption)	4860.973	-2.33E-15 <sup>a</sup>	5.206	20.97
O[III]	5005.22	3.092E-16	0.6974	8.127
Fe[VI]	5158.461	3.642E-16	0.8163	7.648
Mg (absorption)	5176.959	-1.76E-16 <sup>a</sup>	3.927	16.22
Fe[VII]	6084.591	2.387E-16	0.5076	6.632
O[I]	6300.673	3.231E-16	0.7001	11.2
N[II]	6548.056	8.724E-16	1.917	12.9
H <sub>α</sub>	6564.066	5.708E-15	12.81	10.0
N[II]	6584.366	2.947E-15	6.797	11.14
S[II]	6717.033	8.190E-16	2.617	10.92
S[II]	6732.403	6.105E-16	1.964	9.506

(a) The negative sign implies an absorption line.

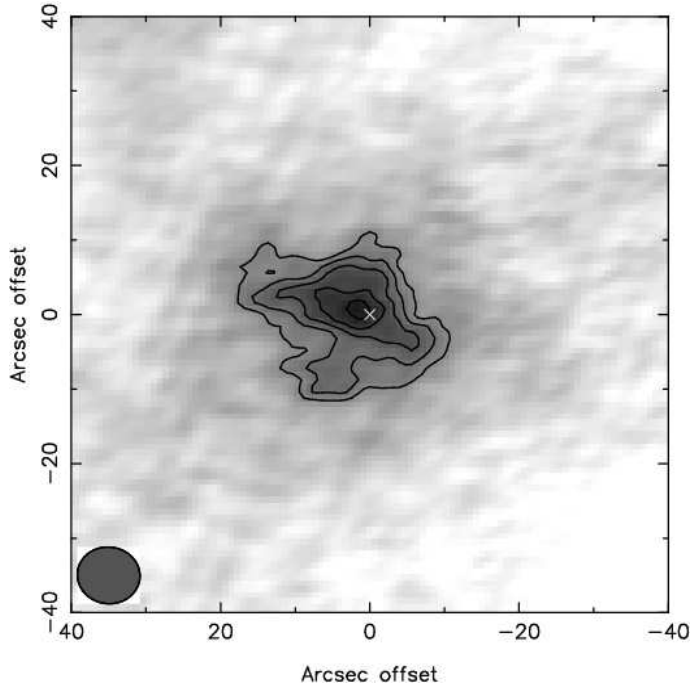


**Figure 1.** Low resolution map of the 1.4 GHz continuum emission from PGC 045080. Natural weighting has been used; the contours are 4, 5, 6, 7 and 8 times the map noise which is 0.085 mJy/beam. The beam is  $8.4'' \times 7.6''$  and the SDSS galaxy center is marked with a cross.

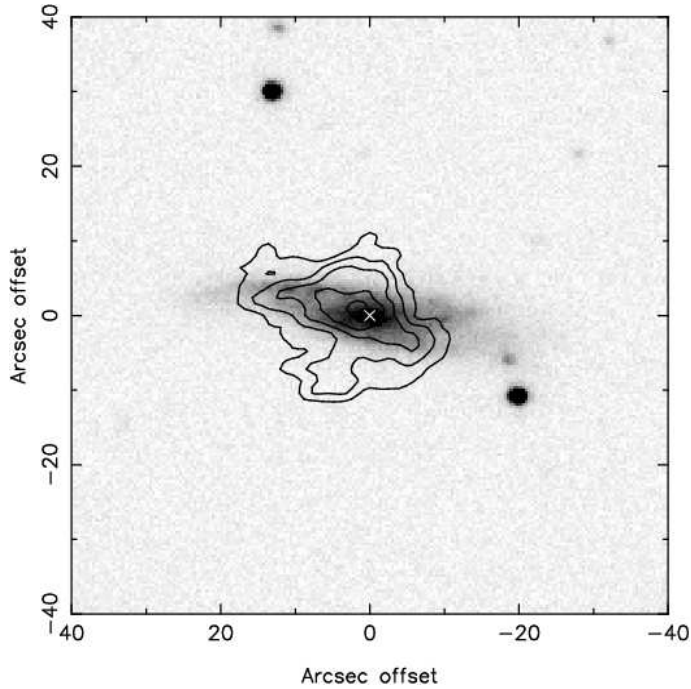


**Figure 2.** SDSS R band image of PGC 045080 with the radio contours of 1.4 GHz emission at low resolution from Figure 2a overlaid. Note that the extended radio emission to the south lies outside the galaxy and is not associated with the galaxy; its origin is unclear.

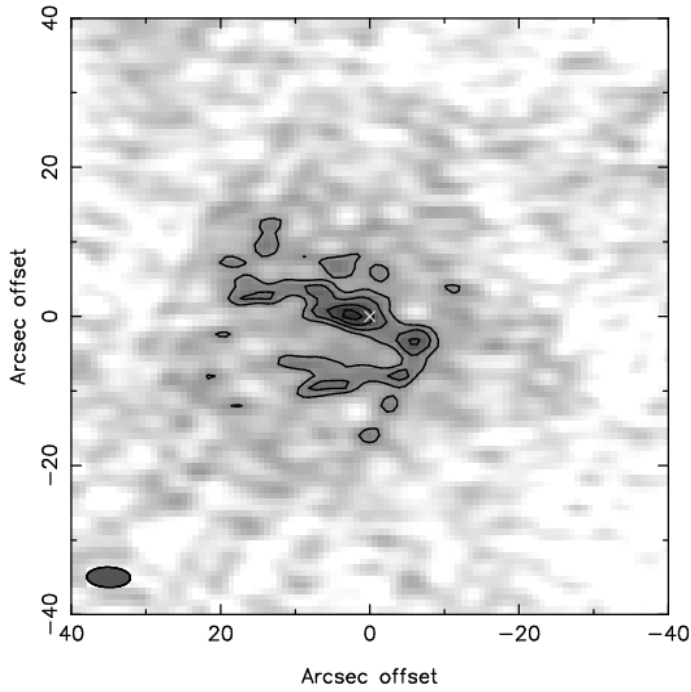


**Figure 3.** Map of the 1.4 GHz continuum emission from PGC 045080. Uniform weighting has been used to make the map and the contours are 3, 4, 5 and 6 times the map noise which is 0.088 mJy/beam where the beam is  $5.9'' \times 2.7''$ . The galaxy center from SDSS is marked with a cross.

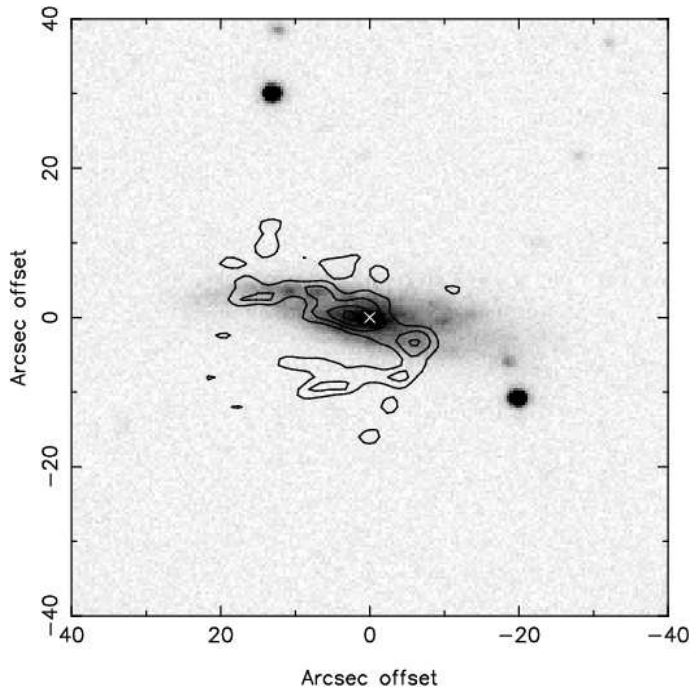


**Figure 4.** SDSS R band image of PGC 045080 with the radio contours of 1.4 GHz emission from Figure 1 overlaid. Note that the P.A. of the radio axis is significantly different from the optical axis.

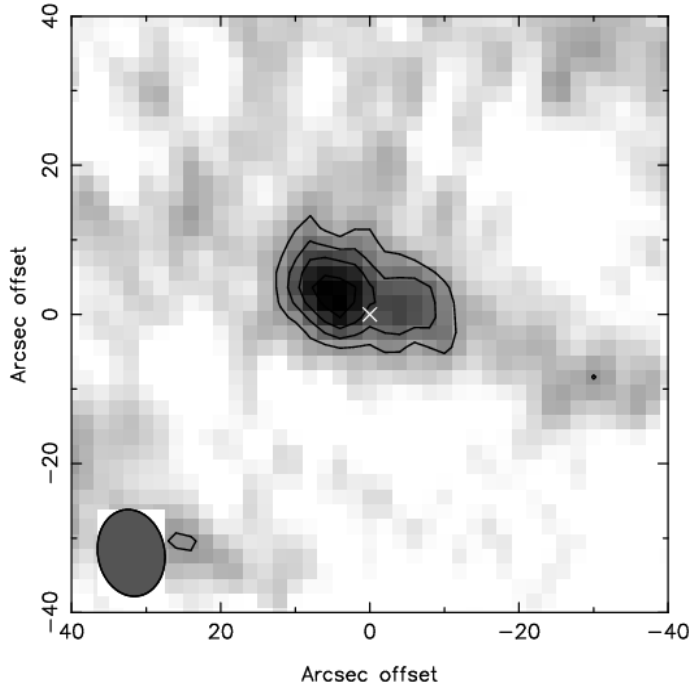


**Figure 5.** The 610 MHz continuum emission map of PGC 045080; natural weighting has been used so the resolution is poor but the sensitivity is relatively higher. The contours are 2, 3, 4 and 5 times the noise level which is 0.16 mJy/beam where the beam is  $11.7'' \times 9.0''$ . The galaxy is detected with a S/N ratio of 6.

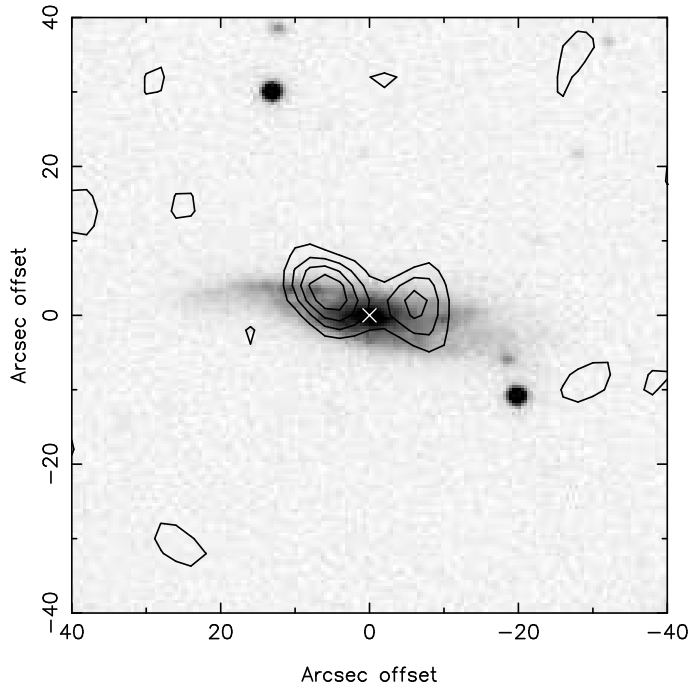


**Figure 6.** SDSS R band image of PGC 045080 with the radio contours of 610 MHz emission map overlaid. The 610 MHz image was made using uniform weighting to achieve better resolution (beam= $7.6'' \times 6.5''$ ). The contours are at 2, 3, 4 and  $5\sigma$  levels where  $\sigma=0.12$  mJy beam $^{-1}$ .

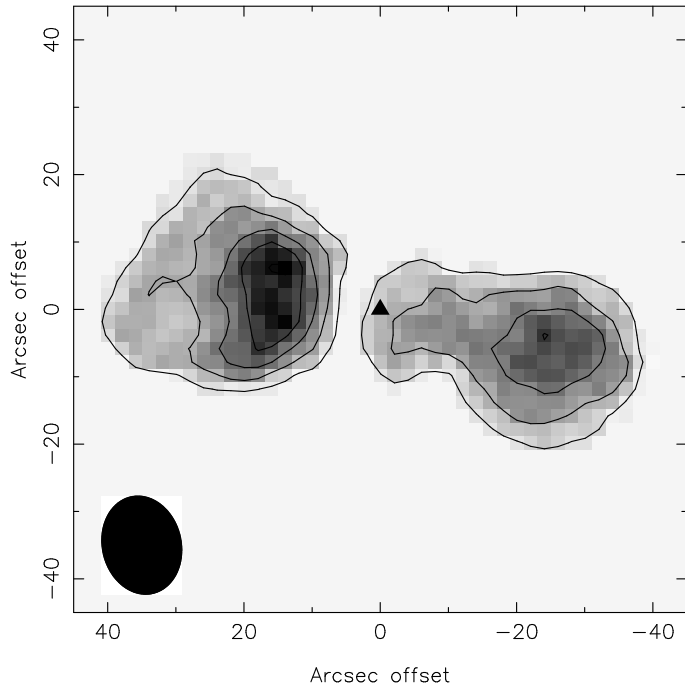


**Figure 7.** Map of the HI intensity distribution in PGC 045080 observed with the GMRT. The contours are at 0.1, 0.3, 0.5, 0.7 times the peak emission which is  $266 \text{ mJy beam}^{-1} \text{ km s}^{-1}$  and the beam is  $14.7'' \times 12.0''$ . Note the gas morphology appears different on either side of the galaxy center.

**Figure 8.** Contours of the HI intensity overlaid on the SDSS R band image of PGC 045080. The HI extent is nearly twice that of the visible optical disk and appears thicker as well.

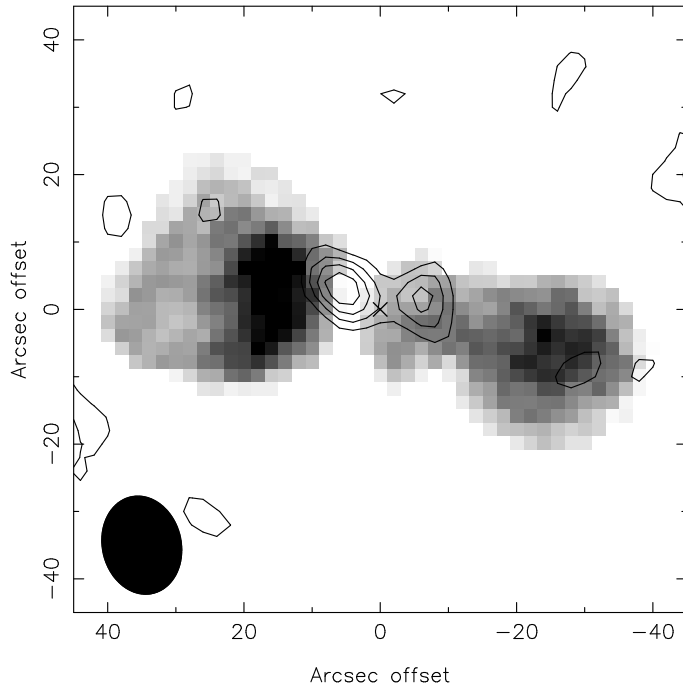


**Figure 9.** Moment zero or HI intensity map of PGC 045080 with the contours of the high resolution 610 MHz emission overlaid. The brighter lobe of the continuum emission coincides with the dip in the HI distribution suggesting that there may have been some jet-cloud interaction in the disk of the galaxy. The contours of the 610 MHz emission is the same as that in Figure 6.

**Figure 10.** Figure shows the HI velocity field field of the galaxy PGC 045080. The velocity contours are spaced  $20 \text{ km s}^{-1}$  apart and are from  $-170$  to  $170 \text{ km s}^{-1}$ , where the central velocity is taken to be the systemic velocity of the galaxy i.e.  $12,264 \text{ km s}^{-1}$ . The contours in green represent the approaching side while (east of the nucleus) while those in black represent the receding side.

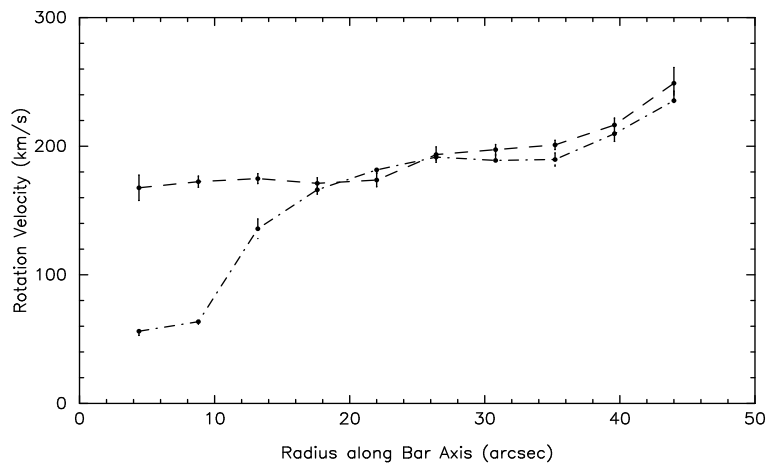


**Figure 11.** The rotation velocities for both sides of PGC 045080 derived from the HI moment map (beam is  $9.2'' \times 8.4''$ ). Nyquist sampling was used and velocities averaged over annuli of width  $\sim 8.8''$ . The approaching side is indicated with a dashed curve and the receding with a dash-dot-dash line. The two sides agree beyond  $20''$  approximately which is the approximate radial extent of the stellar disk.

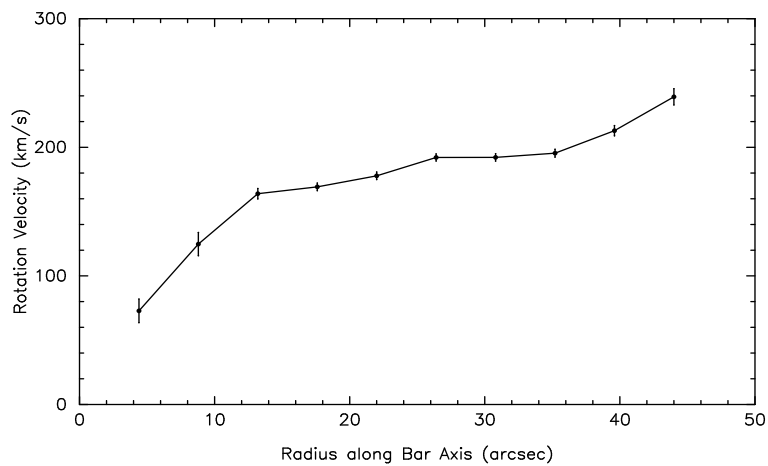


**Figure 12.** The total rotation curve of the galaxy after summing up the contributions from both the approaching and receding sides. The error bar in for each velocity bin is plotted as well. The mean flat rotation velocity is  $\sim 190 \text{ km s}^{-1}$ .

**Figure 13.** The optical spectrum of PGC 045080. The slit was centered on the galaxy center and aligned along the major axis. The main emission lines,  $H\beta$ ,  $O[III]$ ,  $H\alpha$ ,  $N[II]$  doublet and  $S[II]$  are marked on the plot. The Y axis is the flux in  $\text{erg cm}^{-2} \text{s}^{-1}$  and the X axis is the wavelength in Angstrom.

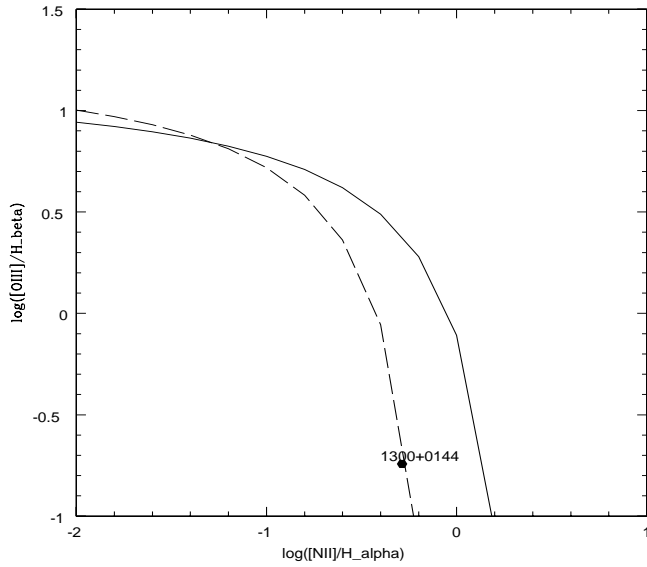


**Figure 14.** Diagnostic diagram of the emission lines from the nucleus of PGC 045080. The solid line gives the limit of extreme starburst (Kewley et al. 2001) and the dashed line is the limit for HII regions from Kauffman et al. (2003). PGC 045080 lies on the border of the dashed line in the lower half of the plot. Hence it may have only a weak AGN, perhaps a LINER type nucleus.

This figure "1300\_mom1\_color2.rot.gif" is available in "gif" format from:

<http://arxiv.org/ps/0705.1417v1>

This figure "1300\_MOM0\_14ARCSEC\_opt.gif" is available in "gif" format from:

<http://arxiv.org/ps/0705.1417v1>

This figure "1300\_spectrum.rot.gif" is available in "gif" format from:

<http://arxiv.org/ps/0705.1417v1>